We are IntechOpen, the world's leading publisher of Open Access books
Built by scientists, for scientists

6,900
Open access books available

185,000
International authors and editors

200M
Downloads

154
Countries delivered to

Our authors are among the

TOP 1%
most cited scientists

12.2%
Contributors from top 500 universities

CLARIVATE ANALYTICS
BOOK CITATION INDEX
INDEXED

WEB OF SCIENCE™

Selection of our books indexed in the Book Citation Index
in Web of Science™ Core Collection (BKCI)

Interested in publishing with us?
Contact book.department@intechopen.com

Numbers displayed above are based on latest data collected.
For more information visit www.intechopen.com

Chapter

Numerical Analysis of Liquid Menisci in the EFG Technique

Sergei N. Rossolenko, Gleb M. Katyba, Irina N. Dolganova,
Irina A. Shikunova, Dmitry O. Stryukov, Kirill I. Zaitsev
and Vladimir N. Kurlov

Abstract

This chapter is devoted to the analysis of the behavior of the profile curves of the melt menisci for the sapphire crystal growth by edge-defined film-fed growth (EFG) technique. The menisci of the shaped crystals with capillary channels, fibers, and tubes (including cases of outer and inner circular menisci) are considered. Also, we investigated the profile curves of menisci both in the cases of the positive and negative angles between profile curve and the working edge of the die. The cases of outer and inner circular menisci of the tubular crystals and menisci at capillaries and fibers are considered.

Keywords: EFG technique, meniscus, profile curve, sapphire

1. Introduction

Single crystalline sapphire has high melting point, chemical inertness, impressive hardness, radiation and mechanical strength, high thermal shock resistance, and thermal conductivity. Sapphire also has high refractive index and a broad transmission band spanning the UV, visible, IR, THz, and microwave bands [1]. Such unique combination of physical and chemical properties makes sapphire an attractive material for various applications.

However, sapphire is difficult to shape because of its high hardness, which makes it difficult or impossible to obtain products of complex shape. In response to this problem, the edge-defined film-fed growth (EFG) technique [2] based on the Stepanov concept [3] was developed. This concept implies that the shape (or an element of the shape) to be produced is formed in the liquid state employing various effects, which enable the liquid to retain the shape. Then, the shape (or element of the shape) is converted to the solid state in appropriate crystallization condition. The method to form a melt column of a defined shape using a special die and to subsequently crystallize the melt column outside the walls of the vessel was suggested. The main idea of this concept is to limit the area of the liquid-free surface and its perturbations.

In the EFG technique, the crystal is grown from a melt film formed on the top of the melt-wettable die, which contains capillary channel (see **Figure 1**). The melt rises to the top of the die due to capillary forces, and the crystal growth proceeds at the top of the die. The edges of the die determine the shape of the meniscus and thus the cross section of the growing crystal. As a result, sapphire-shaped crystals
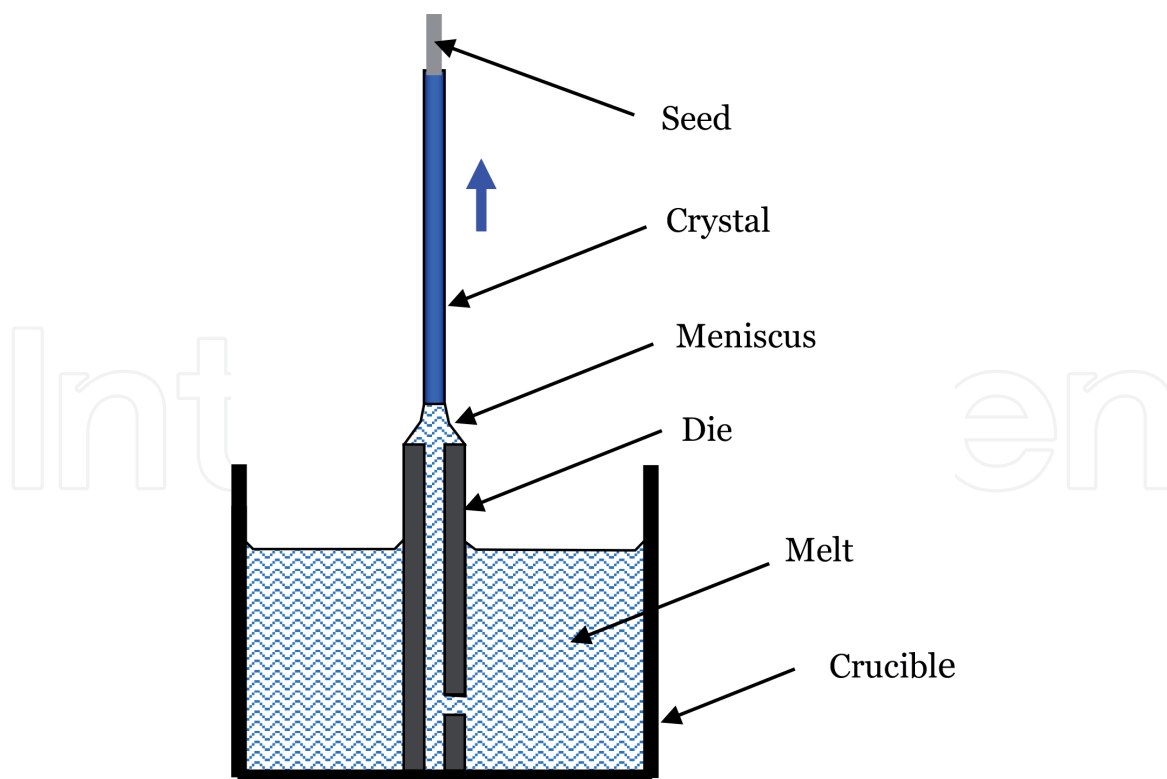
Figure 1.
Schematic of shaped crystal growth by the EFG technique.

of various constant and variable cross sections could be grown by the EFG technique due to its versatility for high-tech applications in optics, material science, biomedicine, etc. [4–10] with the relatively low production cost.

For the EFG technique, shape and quality of crystals are significantly defined by the form and position of the crystallization front and the shape of a liquid meniscus located between a crystal and a die. It is necessary to know the characteristics of the meniscus profile curves for their further use in dynamic models of the crystal-melt system, which are necessary for the development and optimization of automated systems for controlling the growth processes using a weight sensor.

Automated control systems make it possible to control not only the shape of the crystal but also its bulk and surface quality [11, 12], which is extremely important for expanding the fields of application of shaped crystals. In particular, preventing the formation of gas- and solid-phase inclusions in the volume of crystals and a significant improvement in the quality of the growth surface make it possible to use as-grown crystals in optics without additional surface treatment.

There are many publications devoted by the investigation of menisci shape evolution and their influence on the crystallization process. The approximate expression for the height of meniscus connected with the determined boundary conditions is represented in reference [13]. But this expression, usually being applied in Czochralski method, is difficult to use in EFG technique because of interconnected boundary conditions. Detailed consideration of this problem is represented in reference [14]. An approximate expression describing meniscus profile curve for the Czochralski method is given in reference [15]. Investigation of the influence of the negative outer pressure in the melt column of the meniscus on the limits of meniscus height in the crystal pulling of silicon by the EFG method is represented in reference [16]. Detailed research of the melt menisci, in the main, for the positive outer pressures, is given in reference [14]. The heights of menisci providing the implementation of the growth angle permanence condition and

depending on the outer pressure for the sapphire-shaped crystal growth by the EFG method are given in reference [17]. In work [18] the equations for programmed masses of menisci (based on the integration of the Young-Laplace equation and approximate data from the weight sensor signal) for various forms of the crystals' cross section are described. These ones are used in the automated systems of the crystals' form and quality controlling [11] and in consideration of the dynamic models of the crystallization processes [19]. Non-cylindrical (almost quadratic) forms of the meniscus distinguishing for the growth of rare-earth molybdates by modified Czochralski and EFG methods [20] are investigated using numerical solution of the Young-Laplace equation submitted in Cartesian (non-cylindrical) system of coordinates [21]. Thermo-capillary numerical models also require solution of the equation [24–31]. In reference [32] the problem of mechanical stability of the liquid menisci is considered.

This chapter contains the results of study of the profile curves' formation, their properties, and dependence from the various external options and boundary conditions, which determine a meniscus form: outer pressure in the meniscus, height of the meniscus, contact angles between meniscus and working surface of the die, contact angles between meniscus crystal edge, and dimensions of the die and crystal. Variations of the ranges of external options and boundary conditions providing optimal conditions of the crystal growth process are discussed.

Figure 2 illustrates the scheme of meniscus zone for the tubular crystal growth. We consider one (right) side of the vertical cross section of the growing tubular crystal. There are two meniscus profile curves in this cross section—left (inner) and right (outer). The working surface of the die and the crystal edge contact with profile curve via the contact angles θ_d and θ_c, respectively. An angle between a profile line and a tangent line in the corresponding point defines the contact angle. We consider two types of the dies—with horizontal working surface (**Figure 2a**) and with sloped one (**Figure 2b**).

Estimation of the profile curves of the liquid menisci was made using the numerical analysis of the capillary Young-Laplace equation with various options and boundary conditions close to those of the EFG technique. The analysis of the melt-column shaping conditions was made for the case of catching meniscus at working edges of the wettable die. Special mention was paid for menisci providing stationary isotropic growth of sapphire crystal, i.e., profile curve should be satisfied with the condition of the growth angle permanency at the crystal edge (at the triple point). Specified boundary conditions for solving the Young-Laplace equation are close to the real ones resulting in the experimental processes of shaped crystal growth.

In this chapter the following results are presented:

- Analysis of the meniscus profile curves for various cases of catching with die, for various outer pressures, and various sizes of the crystal and the die

- Investigation of the shapes of menisci with negative and positive contact angles

- Analysis of the inner and outer menisci for the tubular crystal

- Analysis of the "planar" menisci for the case of the ribbon

It is well known [22] that the meniscus profile line $z(r)$ for cylindrical crystal and die is defined via capillary Young-Laplace equation in static approximation. For circular meniscus in dimensionless sight, it looks as follows:
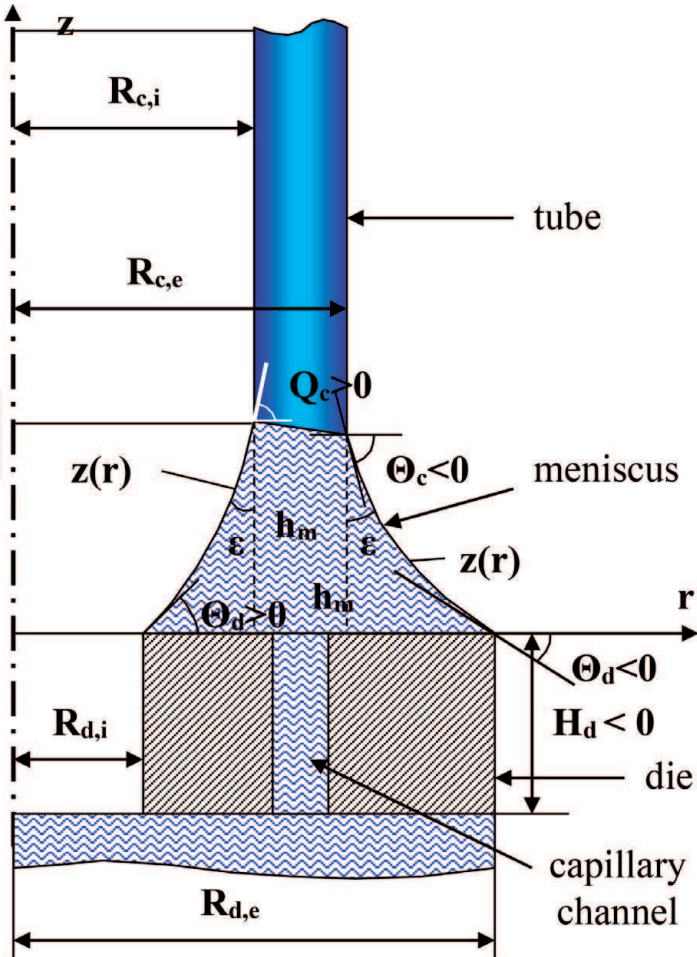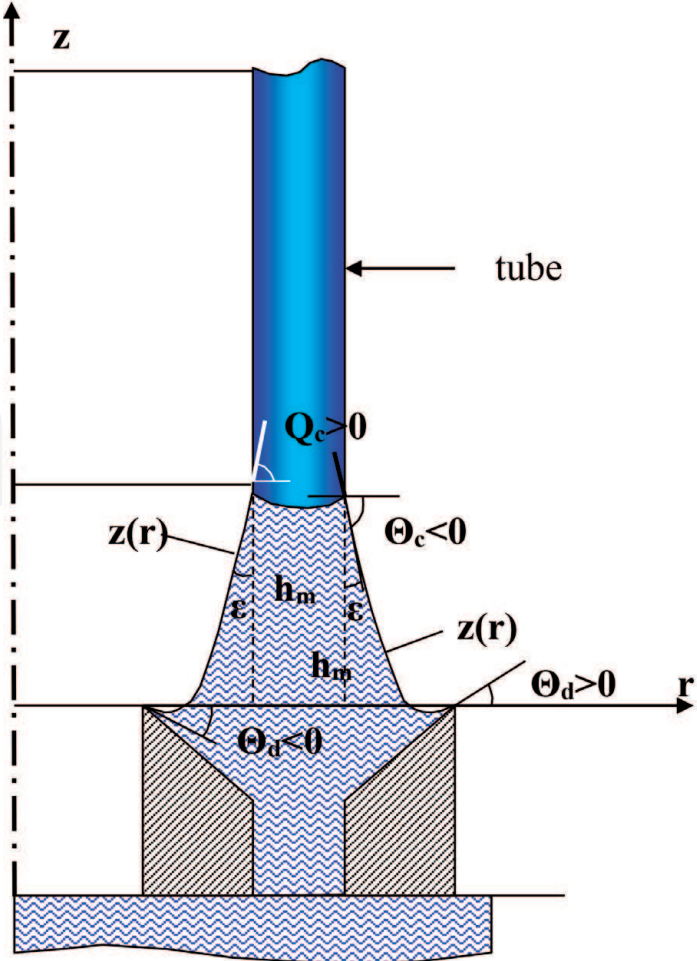
Figure 2.
Schematic of the crystal tube growth (a) with ordinary die and (b) with die having sloped working edges. The right vertical cross-section of the tube is shown.

$$z''r + z'\left(1 + z'^2\right) \pm 2(H_d - z)\left(1 + z'^2\right)^{3/2} r = 0 \qquad (1)$$

where z is current meniscus height, r is current meniscus radius, and H_d is static outer pressure determined mainly by a difference between melt level in the crucible and meniscus base at the working surface of the die.

In sapphire crystal growth by the EFG technique, the base of the meniscus is usually above the melt surface in the crucible, i.e., $H_d < 0$. Thus, in the present chapter, we consider negative outer pressures in the meniscus. For solving the Young-Laplace equation in the case of normal stationary crystal growth, vertical coordinate $z(r)$ is predefined, and horizontal coordinate r is independent from z. Therefore, positive sign before the last part in Eq. (1) is considered. Taking into account the relation between z and r, we can analyze both negative and positive menisci contact angles θ_d between tangent meniscus profile line and horizontal line of the working surface of the die, i.e., the case of ambiguity along the vertical coordinate z is analyzed. In the case of the die with sloped working edge for the outer meniscus of the tubular crystal, a positive contact angle θ_d is possible (**Figure 2b**). In this case, the meniscus of the die is formed along this edge.

In the present chapter, menisci relating to the stationary crystal growth are considered and, hence, being formed without ambiguity along the r coordinate. Therefore, positive sign before the last part in Eq. (1) is considered.

Boundary conditions in our analysis for solving Eq. (1) can be determined as

$$z(R_d) = 0, \; -arctg \; z'\,(r_c) = \pi/2 - \varepsilon \qquad (2)$$

where r_c is a radius of crystal, R_d is a radius of the working surface of the die, and ε is growth angle of the melt (for liquid $Al_2O_3 \approx 13°$ [17, 23]).

Zero height of the meniscus is predefined at the working edge of the die, and for the upper edge of the meniscus, the growth angle should keep permanent.

2. Outer circular menisci

2.1 Analysis of the menisci profile curves for various crystal radii

Numerical data shown in **Figures 3** and **4** were calculated for the outer pressure $H_d = -4$ in dimensionless units. The capillary constant of Al_2O_3 melt is approximately 6 mm [23]. Thus, this outer pressure corresponds to the difference of −24 mm between levels of the melt surface in the crucible and working edge of the die. It is close to data featured to real crystal growth process. Outer pressure is negative because of the upper location of the working edge of the die in comparison with the position of the melt surface in the crucible. The range of crystal radius changing was from 0.95 to 0.995 with step 0.005. We represent linear sizes in dimensionless units in this chapter. In this paragraph the radius of the working surface of the die was constant.

Figure 3a and **b** demonstrates profile curves of the menisci being calculated for the various values of the radius of the cylindrical crystal, i.e., outer right circular menisci of the crystal tube were considered.

As a result of the iterative process, the angle θ_d was automatically adjusted so that the angle θ_c of the meniscus at the point of contact with the crystal (at the triple point) satisfies the condition of constancy of the growth angle. Taking into account the growth angle of sapphire, the required slope angle of the meniscus to the horizontal line at the triple point should be equal to −77° with high accuracy.
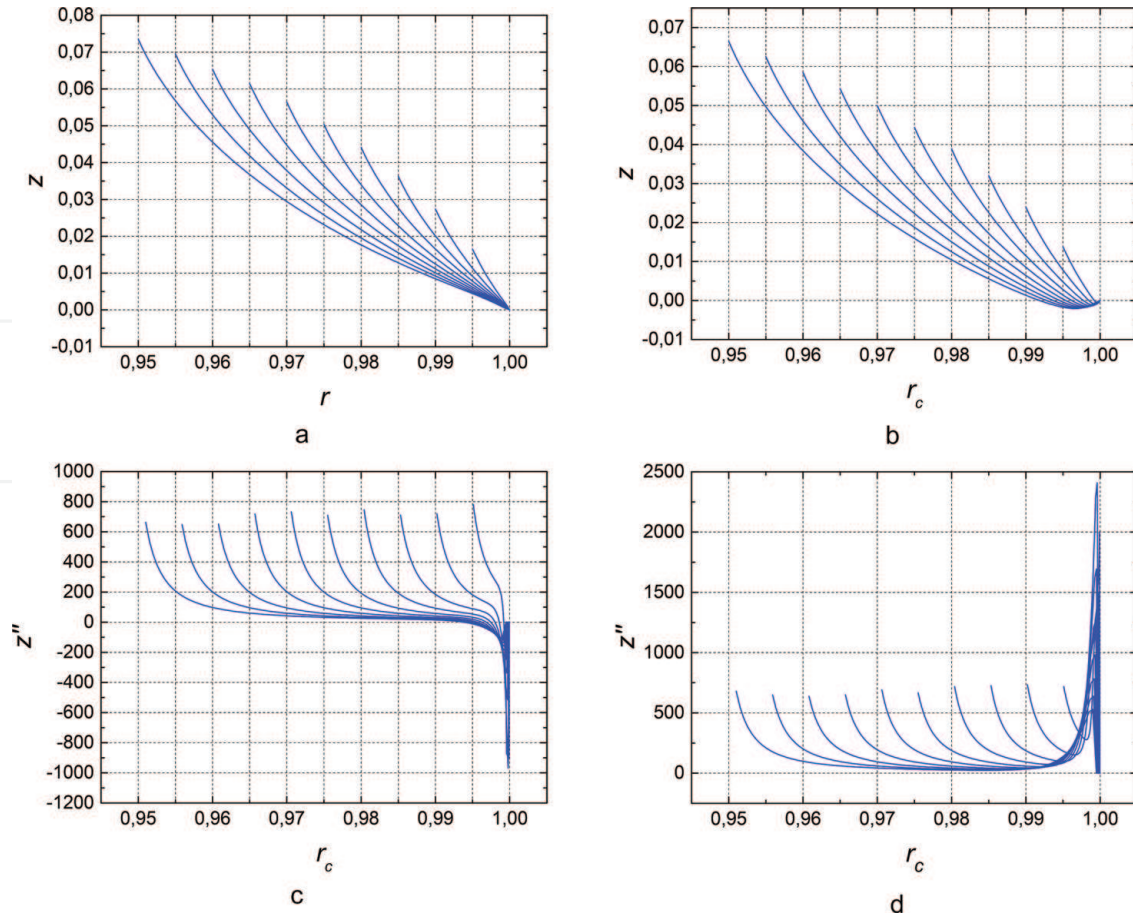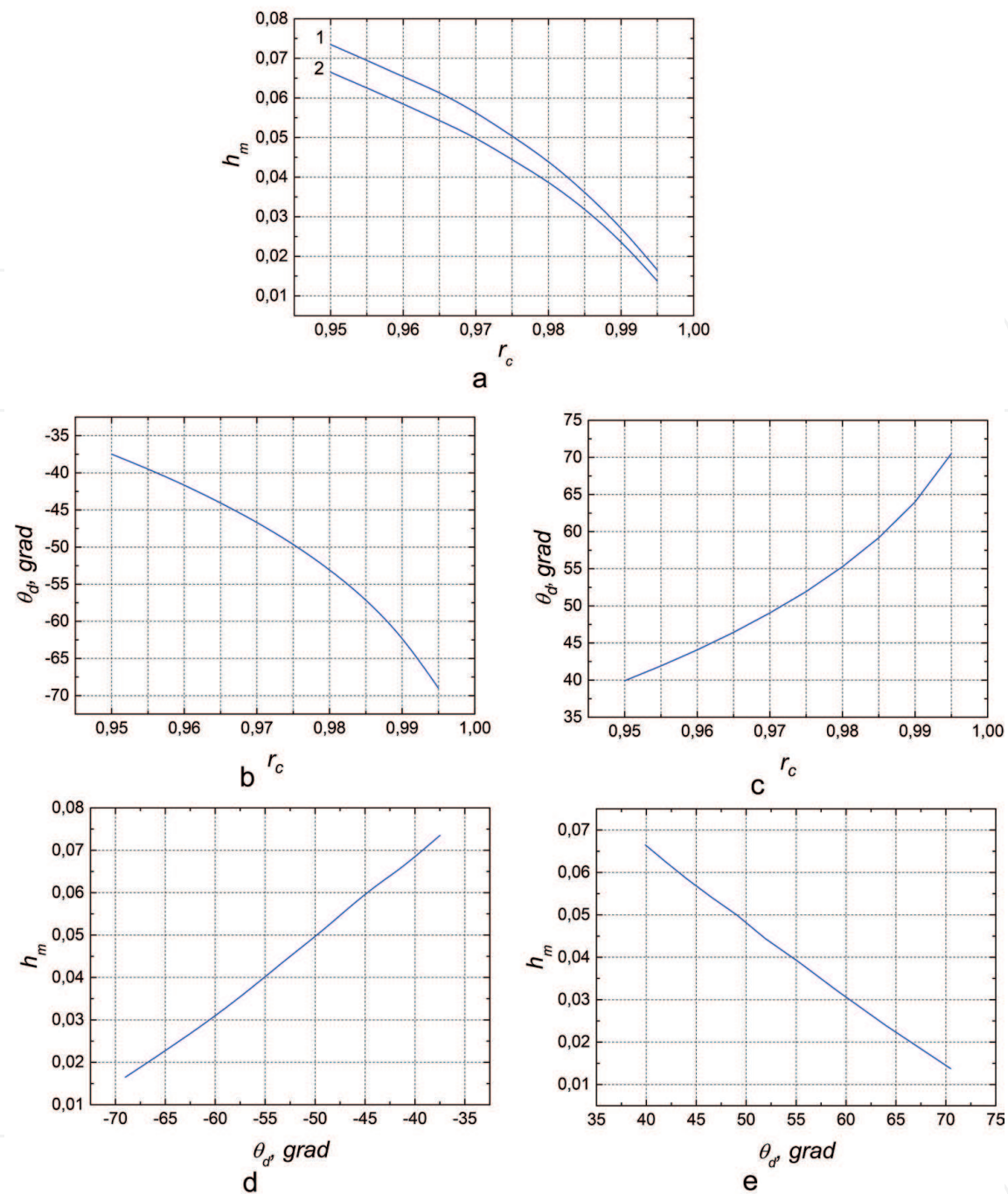
Figure 3.
(a, b) Profile curves of the outer menisci (a) for the negative angles θ_d and (b) for the positive angles θ_d and (c, d) second derivatives of the profile lines of the menisci (c) for the negative angles θ_d and (d) for the positive angles θ_d.

Profile curves depicted in **Figure 3a** correspond to the negative angles θ_d, while in **Figure 3b** to the positive angles θ_d. One can see different shapes of the menisci profile curves in these two cases.

We observe the decrease of the meniscus height with crystal radius increase (**Figure 3a**). With the oncoming of the crystal to the edge of the die, meniscus curves move upward from the die more intensively. There is an upward convexity of the meniscus curves near the die. After the inflection point, a convexity becomes downward.

Meniscus profile curves with positive angles θ_d for the die with sloped working edges are shown in **Figure 3b**. **Figure 3b** demonstrates that the points on the profile curve are displaced down in close proximity to the die and then, as a rule, are displaced upward, toward the edge of the crystal. In both cases, when the radius of the crystal increases, the behavior of the menisci is similar. Thus, if we change the angle θ_d from $-\pi/2$ to $+\pi/2$, the Young-Laplace equation has two solutions satisfying the boundary conditions (2): for the positive and negative angles θ_d.

The second derivatives of the meniscus profile curves are demonstrated in **Figure 3c** and **d**. The second derivatives characterize a curve convexity direction. Negative second derivatives near the die for negative contact angle (**Figure 3c**) correspond to a bulge upward. With the rise of the meniscus height, the second derivative becomes positive. This corresponds to a bulge of the meniscus profile curve downward. Thus, the second derivatives grow as the profile curve approaches the edge of the crystal. This shows that the convexity of the profile curves increases near the edge of the crystal.

Figure 4.
(a) The curves of the meniscus height depending on the crystal radius (first line) for the contact angles $\theta_d < 0$ and (second line) for the contact angles $\theta_d > 0$, (b, c) the curves of the contact angle θ_d depending on the crystal radius (b) for the angles $\theta_d < 0$ and (c) for the angles $\theta_d > 0$, (d, e) the lines of meniscus height depending on the contact angle θ_d (d) for the angles $\theta_d < 0$ and (e) for the angles $\theta_d > 0$.

The second derivatives of the meniscus profile curves for positive angles θ_d (see **Figure 3d**) have a positive sign everywhere along the current radii of the meniscus. The values of the second derivatives near the crystal are significantly larger than at a sufficient distance from it. In the case of positive angles θ_d, the inflection point is absent, and menisci have convexity everywhere in melt direction.

Figure 4a demonstrates dependence of the height of the meniscus on the radii of the crystal. We observe diminishing meniscus height with crystal radius rise (**Figure 4a**) and its oncoming to the edge of the die. Decrease of the meniscus height corresponds to smaller height of the interface boundary. This corresponds to

colder thermal zone of the system "melt-crystal." In a growth process, it is necessary to choose some middle position of the interface boundary corresponding to the optimal conditions for crystal formation.

Figure 5 shows the surface of dependence of the outer meniscus height on the outer pressure and the radius of the die for the case of the negative angle θ_d and for the crystal tube outer radius 0.97 (in capillary constants).

2.2 Influence of various outer pressures on the menisci profile curves

We have made the calculations for various pressures being changed from -8 to 0 with step 1 in capillary constants (dimensionless units) via the constant die and crystal radii equal to 1 and 0.97, respectively. The requirement of growth angle permanence was satisfied during calculations.

With the rise of outer pressure in the range from $H_d = -8$ to $H_d = 0$ the meniscus height increases (**Figure 6a, b**). It takes place because of diminishing the force pressing meniscus down to the die.

As shown in **Figure 7a**, meniscus height decreases with the rise of absolute value of outer pressure for negative contact angles as well as for positive ones. Therefore, **Figure 7** shows the features of the meniscus profile lines only for negative boundary angles θ_d.

Diminishing the absolute value of the outer pressure increases the absolute value of the contact angle θ_d (**Figure 7b**). To obtain the appropriate (higher) meniscus height, the larger absolute values of contact angles θ_d are required (**Figure 7a** and **b**). The function of the meniscus height depending on the boundary angle θ_d is almost linear (**Figure 7c**).

2.3 Influence of various boundary angles θ_d on the menisci profile curves

We have made analysis for the various boundary angles θ_d, while the die and crystal radii were constant. The die radius was equal to 1, crystal radius was equal
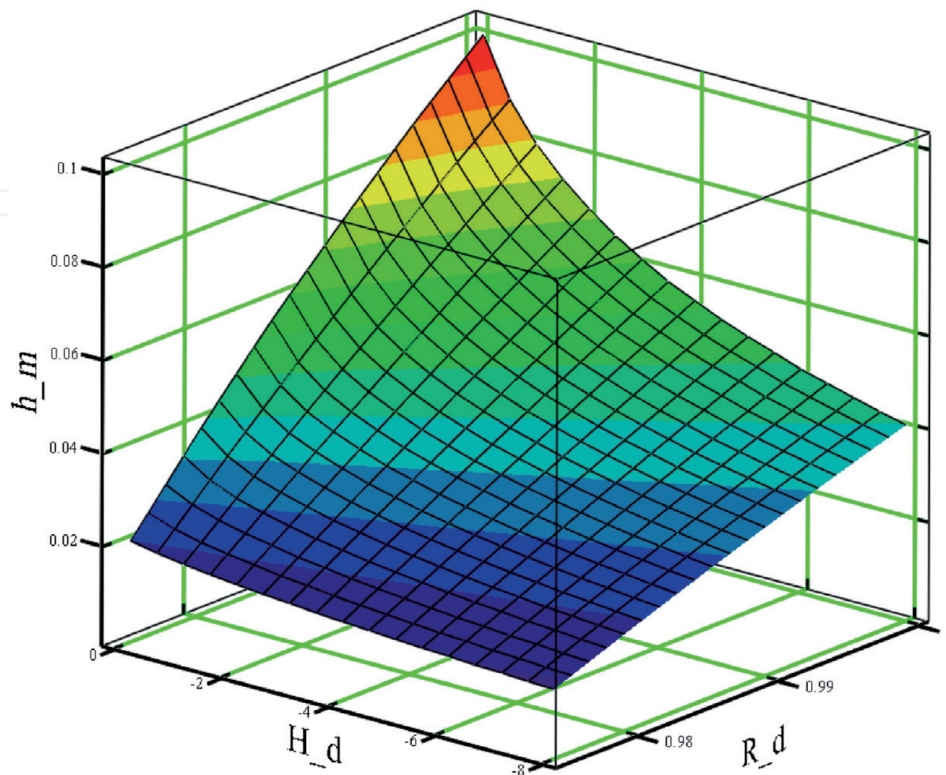
Figure 5.
The surface of dependence of the meniscus height on the outer pressure and the radius of die.
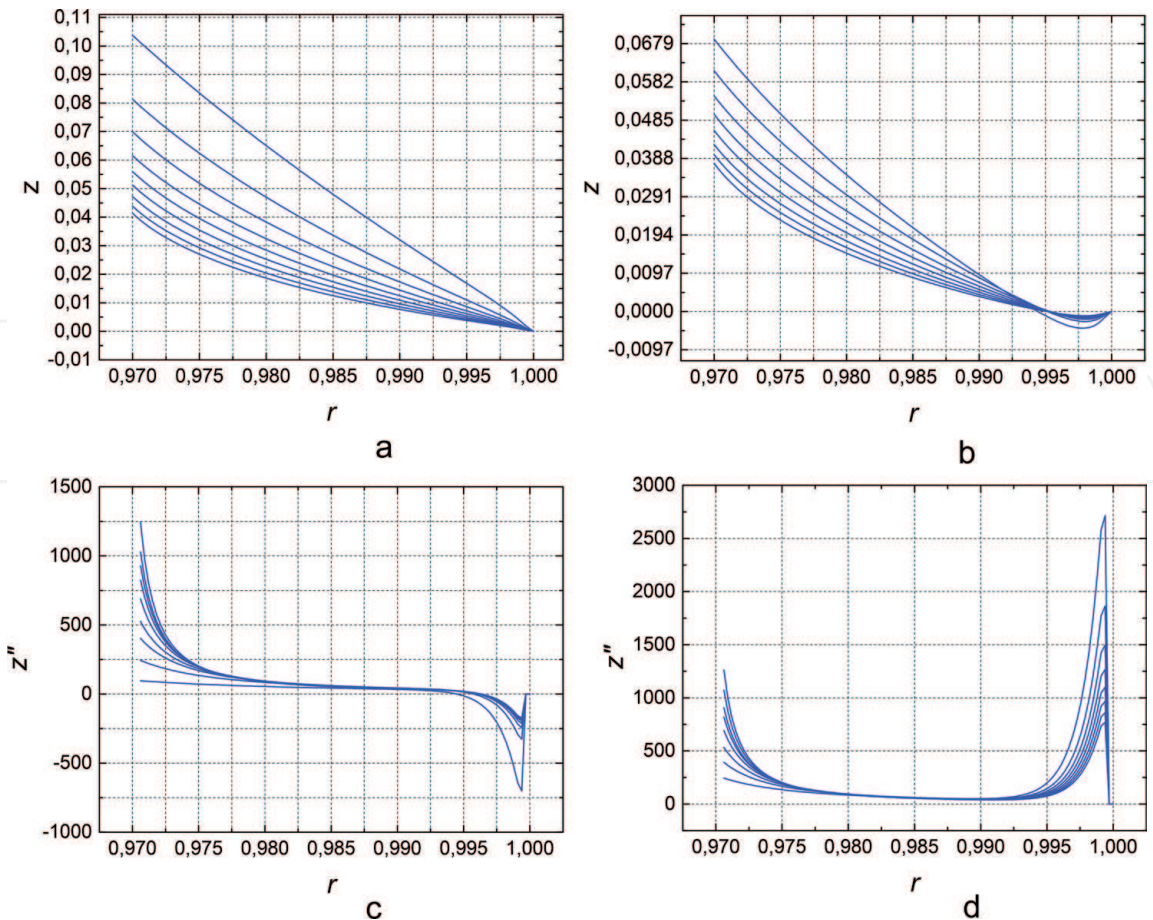
Figure 6.
(a, b) Profile curves of the menisci for the various outer pressures (a) for the negative angles θ_d and (b) for the positive angles θ_d and (c, d) second derivatives of the profile curves of the menisci for the various outer pressures (c) for the negative angles θ_d and (d) for the positive angles θ_d.

to 0.97, and outer pressure was equal to −4, in dimensionless units (capillary constants). Requirement of the growth angle permanence at triple point was not satisfied. We have used the next boundary condition:

$$z(R_d) = 0, \ arctg \ z'(R_d) = \theta_d \qquad (3)$$

Figure 8a shows that the large absolute values of the boundary angles θ_d result in significantly higher menisci. Diminishing and rise of line segments (**Figure 8a**) correspond to the case above. Derivatives of the line decrease and rise is significant. Hence, the range of the menisci heights being sufficient for the stable growth and being satisfied with the condition of the growth angle permanence is sufficiently narrow. **Figure 8b** demonstrates that the ranges of boundary angles being almost real are approximately from −50 to −30° for the negative boundary angles θ_d and from +30 to +50° for the positive ones.

Under relatively small absolute values of the boundary angles (<30°), θ_d menisci heights are very small and unreal in a course of the sapphire crystal pulling by EFG technique.

2.4 Influence of various values of die and crystal radii (with constant difference between them) on the features of menisci

We have considered simultaneous changing of the die and crystal radii with constant distance between them, which was equal to 0.03 in dimensionless units (capillary constants).
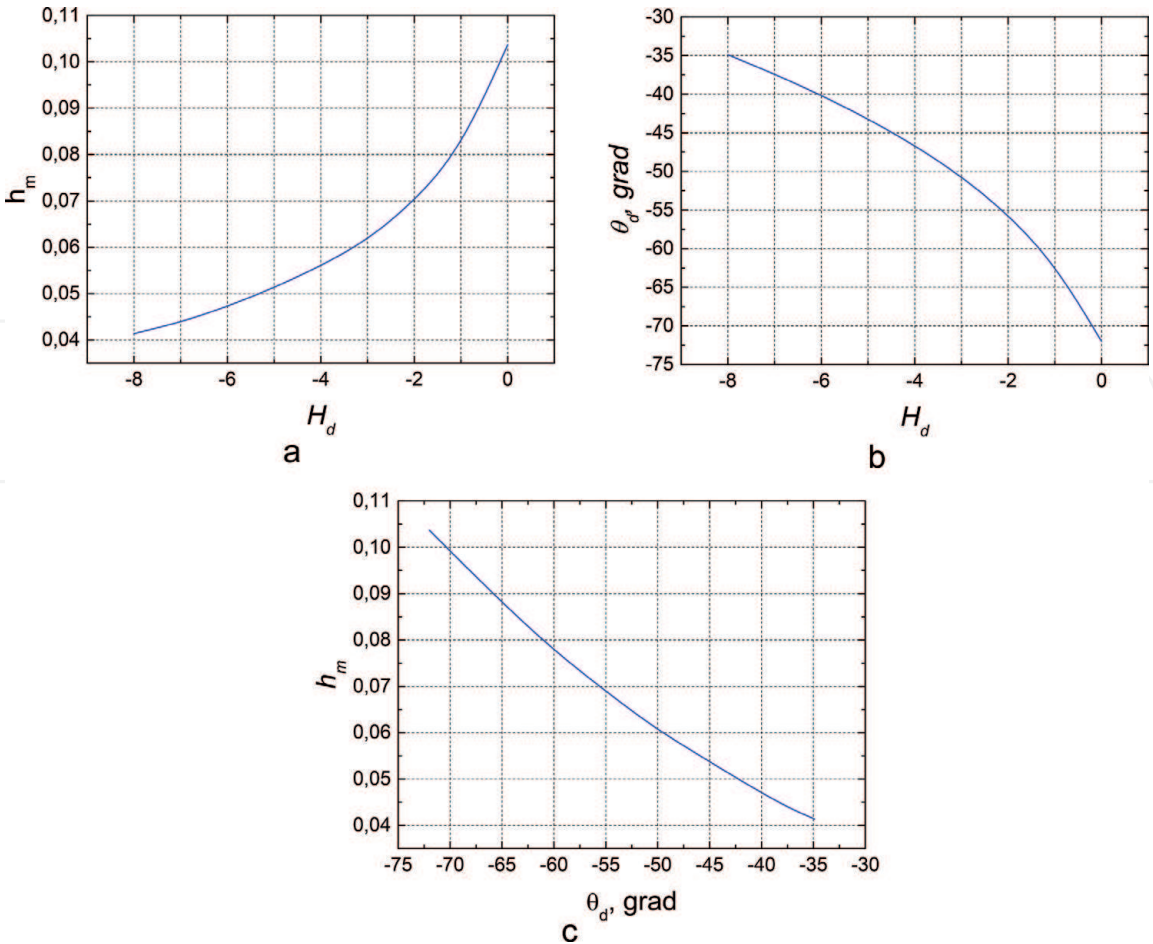
Figure 7.
(a) Function of the meniscus height depending on the outer pressure, (b) function of the boundary angle θ_d depending on the outer pressure, and (c) function of the meniscus height depending on the boundary angle θ_d.
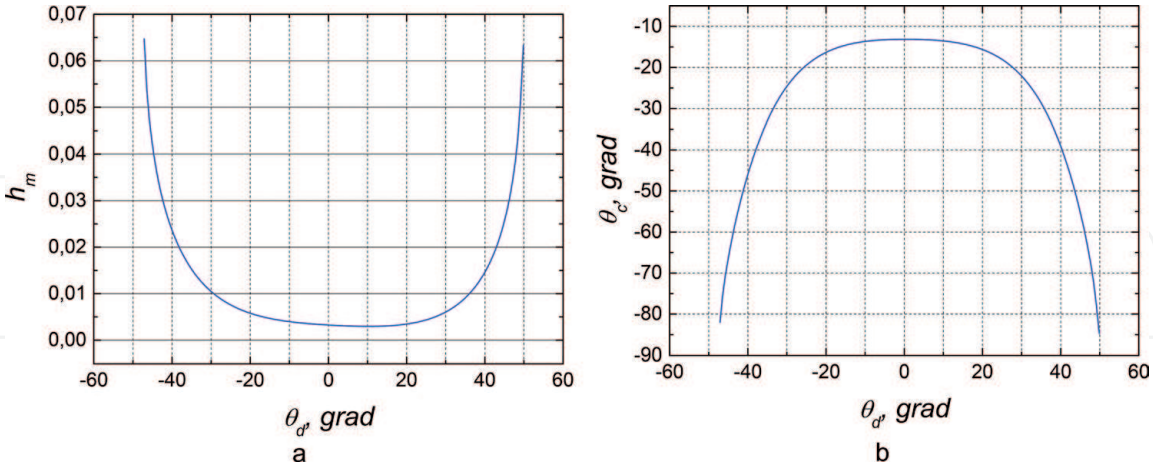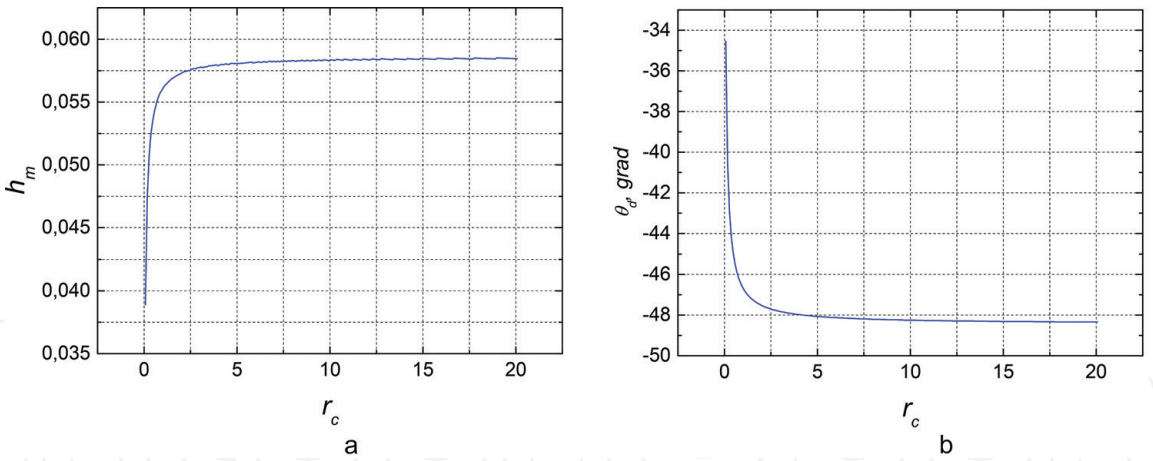

Figure 8.
(a) Function of the meniscus height depending on the boundary angle θ_d and (b) function of the boundary angle θ_c depending on the boundary angle θ_d.

The die radius was changing from 0.1 to 20, and the crystal radius was changing from 0.07 to 19.97. For sapphire it corresponds to the change from 0.42 mm to approximately 120 mm of crystal radius. We took into account the requirement of the growth angle permanence at the crystal edge.

Figure 9a shows that the strong changing of the meniscus height takes place at the die and crystal radii change at sizes of the capillary constant. The same situation is also for the change of θ_d (**Figure 9b**).

Figure 9.
(a) Function of the meniscus height depending on the crystal (and die) radius for the tubular crystal and (b) function of the contact angle θ_d depending on the crystal (and die) radius for the tubular crystal.

3. Inner menisci for the tubular crystal

We have analyzed the inner menisci for the tubular crystal with similar data as for outer menisci. **Figure 10** shows typical profile lines of the inner menisci. There are some differences connected with the fact that azimuthal curvature (second part of the capillary Eq. (1)) has positive sign for the inner meniscus and negative sign in the case of outer meniscus.

This curvature enlarges the current meniscus height due to the positive sign of the azimuthal curvature for the inner menisci. Profile curves of the inner menisci are a little bit higher than outer menisci due to the positive sign of the azimuthal curvature. This results in the presence of additional compressing factor in the inner menisci.

We have also considered simultaneous change of the die and crystal radii with constant distance between them. Outer pressure H_d was equal to -4 in dimensionless units (capillary constants). Requirement of the growth angle permanence in triple point was implemented.

The dependence of the meniscus height on the crystal and die radii (**Figure 11a**) has difference in comparison with the one in the case of the outer circular menisci and has opposite behavior. The line of the inner menisci height is slightly diminishing, but outer menisci height rises. This can be explained by the opposite signs of the azimuthal curvature.
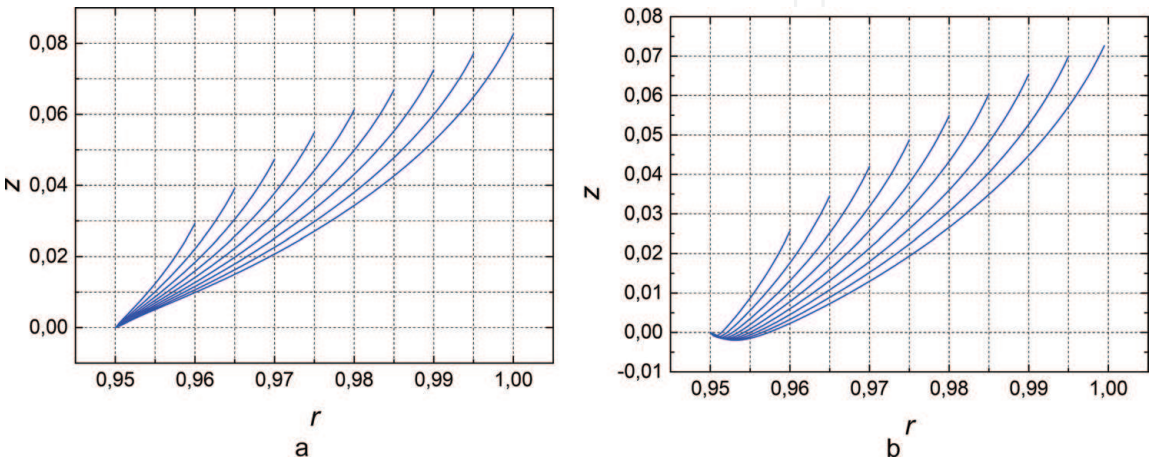
Figure 10.
(a, b) Profile lines of the inner menisci (a) for the positive angles θ_d and (b) for the negative angles θ_d.

11
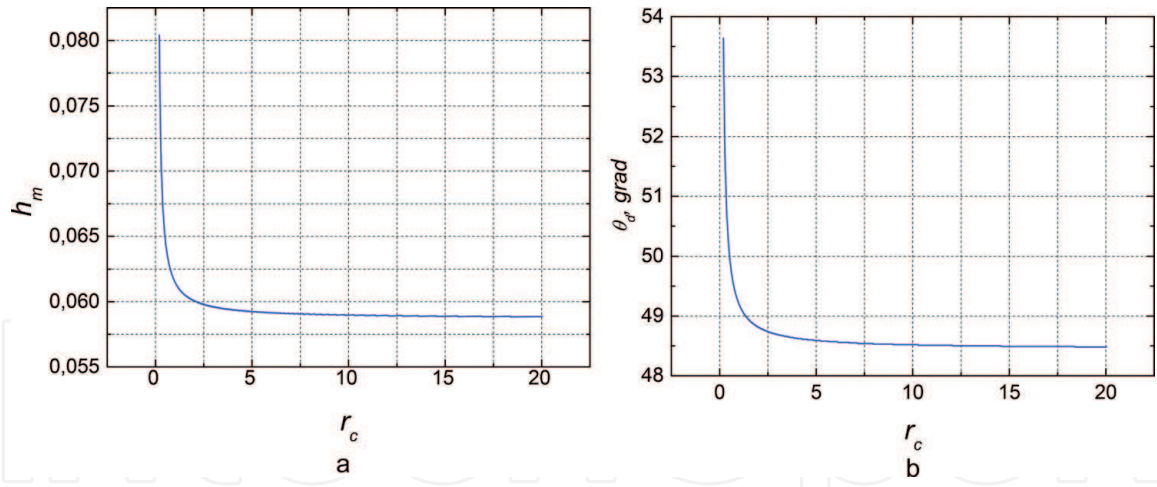
Figure 11.
(a) Function of the meniscus height depending on the crystal (and die) radius for the inner circular menisci and (b) function of the contact angle θ_d depending on the crystal (and die) radius for the inner circular menisci.

We have considered also "planar" menisci being formed at the wide side of the crystal ribbon. The Young-Laplace equation was analyzed with zero azimuthal curvature. Using the same modeling options (as for circular menisci), we have found that the heights of "planar" menisci are a little bit higher than the heights for the outer circular menisci and a little bit lower than the heights for the inner menisci. This can be explained by zero azimuthal curvature. The influence of the various outer pressures, various crystal ribbon width, and other factors is the same as for the circular menisci.

4. Application of menisci analysis to automated control in EFG technique

The programmed expression of observing for weight sensor is necessary for automated control in EFG technique. At periods of control, the mass being calculated via this expression is compared with real signal of the weight sensor. Obtained deviation is used for calculation of regulating impact in the feedback closed loop of control process.

For the stationary tubular crystal growth with quasi-planar crystallization front, the meniscus part of the observing expression should be written as follows [12, 18]:

$$M_m = \pi\rho_L\left(r_{c,e}^2 - r_{c,i}^2\right)\left(h_{m,e} + h_{m,i}\right)/2 - 2\pi\rho_L a^2 r_{c,e} sin\theta_{c,e} + 2\pi\rho_L a^2 r_{c,i} sin\theta_{c,i}$$
$$+ 2\pi\rho_L a^2 R_{d,e} sin\theta_{d,e} - 2\pi\rho_L a^2 R_{d,i} sin\theta_{d,i} - 2\pi\rho_L\left(R_{d,e}^2 - R_{d,i}^2\right) H_d \qquad (4)$$

Here, $r_{c,i}$ is a radius of the tube inner side, $r_{c,e}$ is a radius of the tube outer side, $R_{d,i}$ is a radius of the die inner working edge, $R_{d,e}$ is a radius of the die outer working edge, $h_{m,i}$ is an inner meniscus height, $h_{m,e}$ is an outer meniscus height, $\theta_{c,i}$ is a contact angle of the inner meniscus with the crystal edge, $\theta_{c,e}$ is a contact angle of the outer meniscus with the crystal edge, $\theta_{d,i}$ is a contact angle of the inner meniscus with die working surface, $\theta_{d,e}$ is a contact angle of the outer meniscus with the die working surface, ρ_L is a density of the melt, a is a capillary constant, and H_d is an outer static pressure.

The angle θ_c is connected with growth angle and specific for each liquid material. The outer pressure can be calculated from the dimensions of crucible and die and
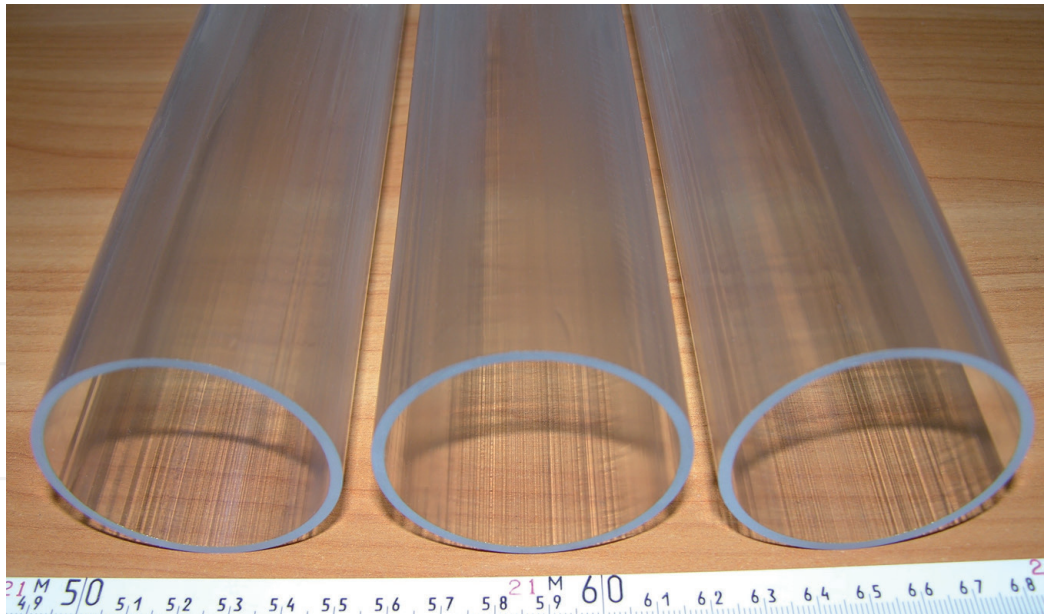
Figure 12.
Sapphire tubular crystals of 55 mm in outer diameter grown by EFG technique using automated control system.

total melt charge in the crucible. The programmed menisci heights and angles of contact with working surface of die can be calculated from solution of the Young-Laplace equation.

For the known outer pressure and growth angle, we can find menisci heights and angles of contact with the die, using **Figures 7b** and **8a**. Similar estimations can be made for inner as well as for outer menisci.

The optimal heights of inner and outer menisci and, hence, optimal conditions at the crystallization front are necessary to grow sapphire tubular crystals of high quality. To reach this purpose, die top design and special thermal shields are used [33].

We have grown large-scale sapphire tubular crystals of 55 mm in the outer diameter (**Figure 12**) using optimal values of menisci heights and contact angles in the automated control system.

## 5. Small inner menisci for tubular crystals (at capillary)

We have analyzed small inner menisci of capillaries for various crystal radii for the outer pressure $H_d = -4$ in dimensionless units (capillary constants). We changed the crystal radius from 0.05 to 0.0486 with step -0.0002. For sapphire it corresponds to the change from 0.3 to 0.2916 mm with step -0.0012 mm. The radius of the die edge was equal to 0.0485 (in dimensionless units) or 0.291 mm. We have made calculations for the positive contact angles θ_d.

As shown in **Figure 13a**, menisci profile lines have another character in comparison with lines demonstrated in **Figure 3a** shown above for sufficiently "large" menisci. As mentioned above, it is connected with the fact that azimuthal curvature has positive sign in the case of inner meniscus and negative sign in the case of outer meniscus.

As shown in **Figure 13a**, capillary menisci have an upward convexity. It takes place because of the very small weight and sufficiently large value of azimuthal convexity. The heights of capillary menisci are sufficiently small because of the small sizes of crystal radii (**Figure 13b**).
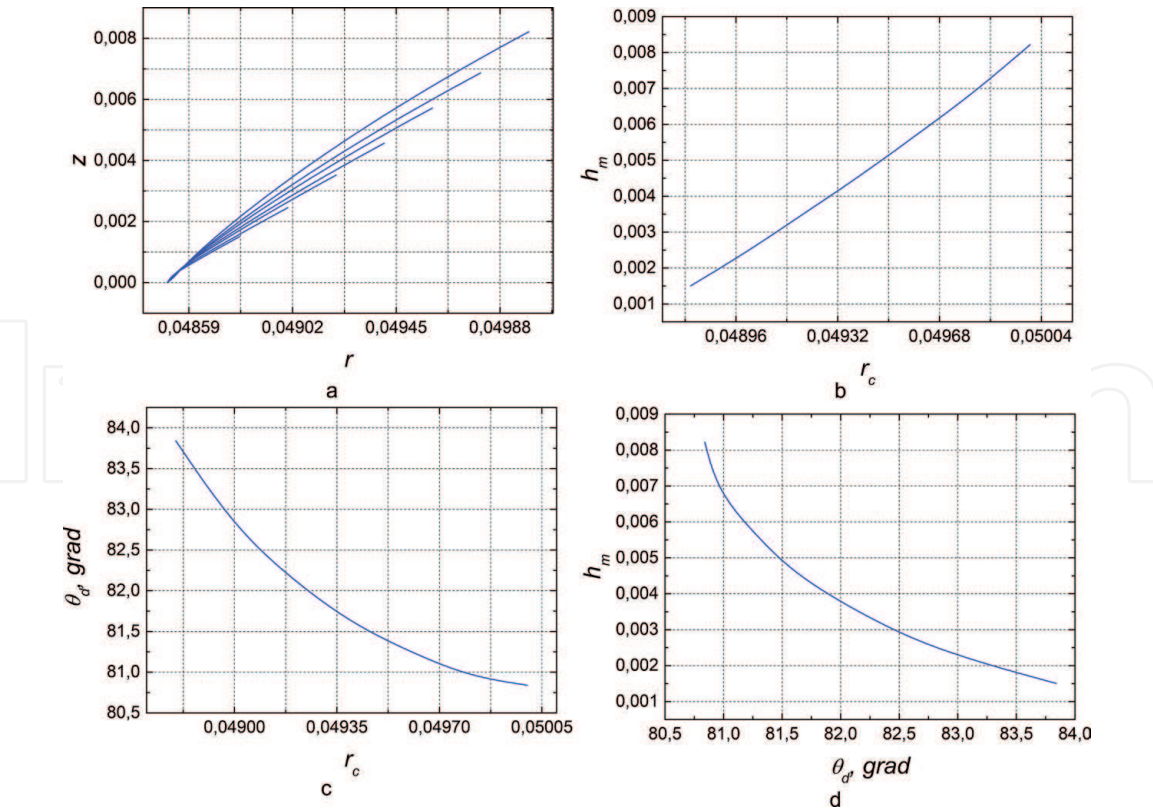
Figure 13.
(a) Profile lines of the small inner capillary menisci at the various crystal radii, (b) function of height of the capillary menisci depending on capillary radius, (c) function of the angle θ_d depending on the capillary radius, and (d) function of height of the capillary menisci depending on the angle θ_d. Positive angles θ_d are considered.
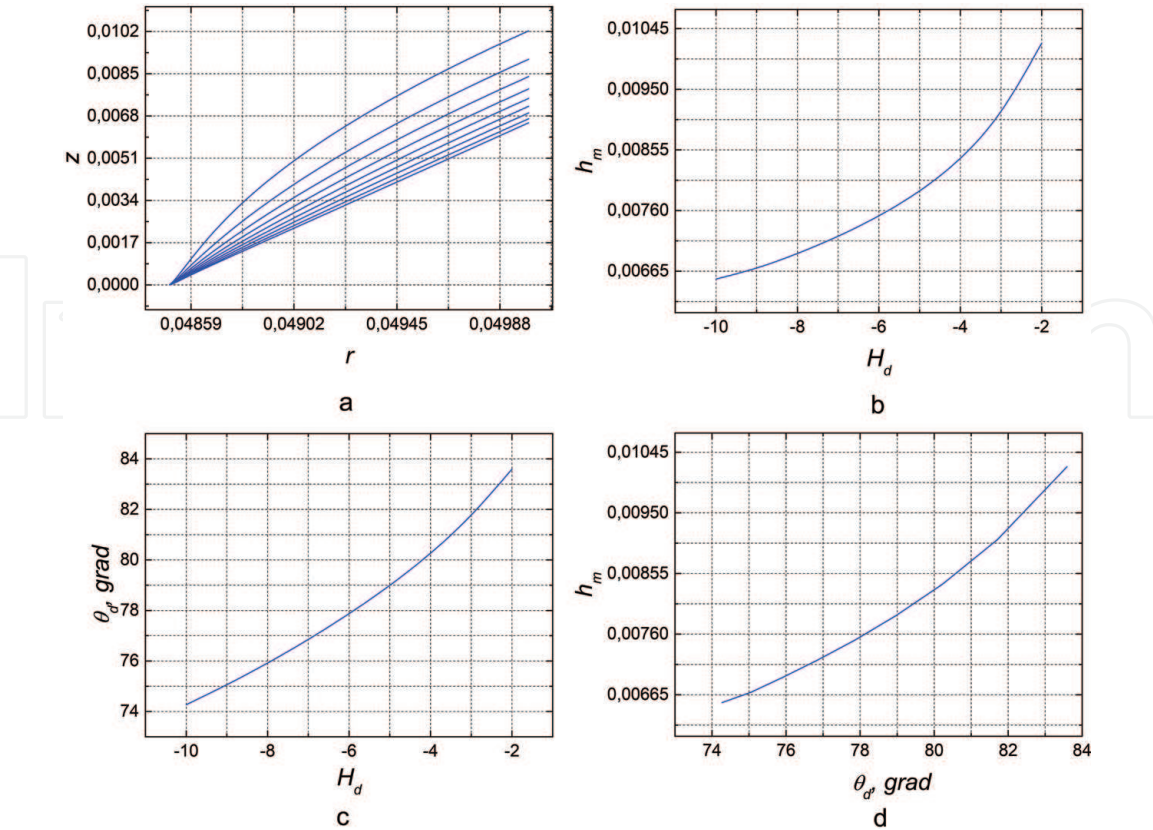
Figure 14.
(a) Profile lines of the small inner menisci (at capillaries) for the various outer pressures, (b) function of the meniscus height depending on the outer pressure, (c) function of the angle θ_d depending on the outer pressure, and (d) function of the meniscus height depending on the angle θ_d at various outer pressures.

For capillary menisci, absolute values of the contact angles (**Figure 13c**) are significantly larger than for the "large" menisci. For the small menisci, larger angles θ_d are required, because the form of small profile lines has convexity directed upward, differing by this from the form of the "large" menisci.

For the small menisci, dependence of the meniscus height on the angle θ_d (**Figure 13d**) is nonlinear compared with "large" menisci. It takes place due to the upward convexity of the capillary menisci.

The die radius was 0.0485, and crystal radius was 0.05 in investigation of the capillary profile lines for the various outer pressures. The value of the outer pressure was changed from −10 to −2 with step 1. Calculations have been fulfilled for the positive angles θ_d.

As demonstrated in **Figure 14**, the capillary meniscus height becomes smaller with rise of the absolute value of the outer pressure as in the case of "large" menisci.

6. Small menisci for fibers

We have made the investigation of the profile lines of the small (outer) fiber menisci variating the crystal radii under the outer pressure $H_d = -4$ (in dimensionless units). We were changing the crystal radius from 0.0483 to 0.0499 with step 0.0002. For sapphire it corresponds to the change from 0.290 to 0.2994 mm with step 0.0012 mm. The radius of the die working surface is equal to 0.05 (in dimensionless units) or approximately 0.3 mm. The negative boundary angles θ_d have been considered.

Due to another sign of the azimuthal curvature, the form of the fiber menisci strongly differs from the capillary ones (**Figure 15**).

We have made analogous numerical analysis for small fiber menisci as for the case of the "large" outer menisci (**Figure 5**). As a whole, behavior of the small fiber menisci and their features are similar to behavior of the "large" outer menisci for the tubular crystals (**Figure 16**).
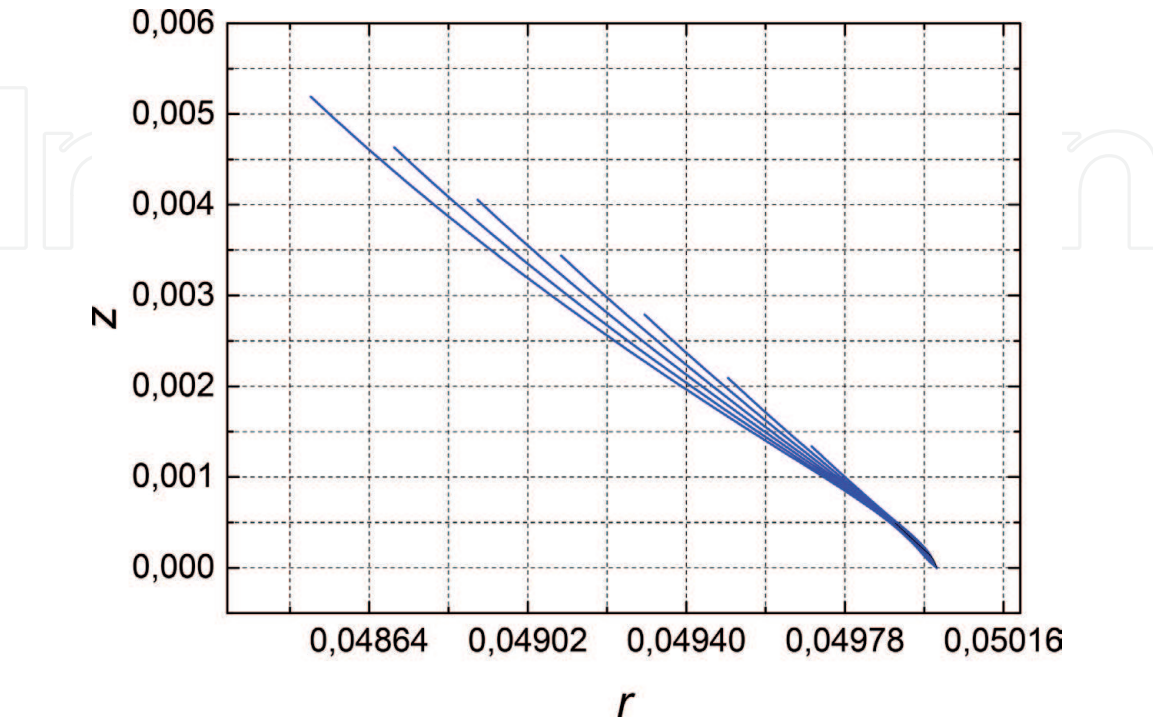
Figure 15.
Profile lines of the small (outer) fiber menisci at various crystal fiber radii. Negative angles θ_d are considered.
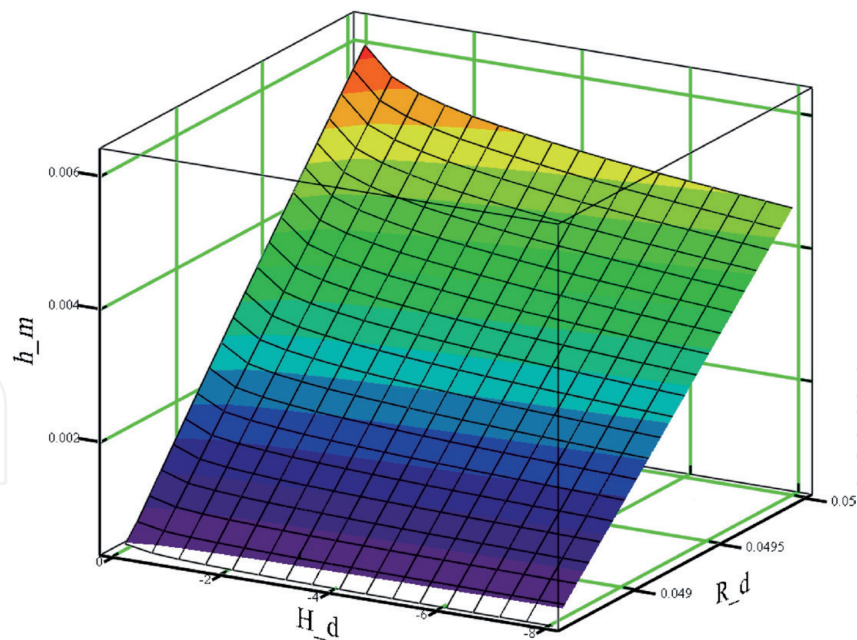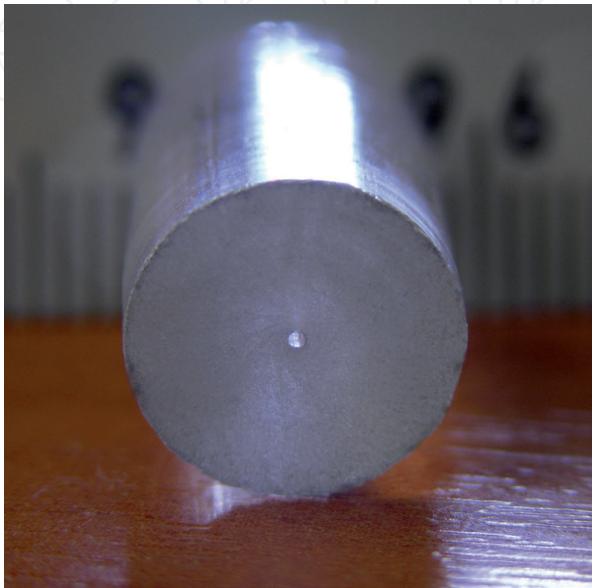
Figure 16.
The surface of dependence of the small meniscus height on the outer pressure and the radius of die.

7. Application of small menisci analysis to sapphire fibers and capillaries' growth using automated control

The data calculated from numerical solution of the Young-Laplace equation for the fibers and capillaries as well as for the large crystals are used in the programmed expression of observation of the weight signal. Due to the deviation between the programmed data and the weight signal, there are first and second derivatives of the deviation calculated that form the signal for heating power by the proportional-integral-differential (PID) procedure.

Automated system also observes the amplitude of the first derivative of the weight signal deviation. The sufficiently strong amplitude corresponds to over-cooling in the thermal zone, and sufficiently small amplitude corresponds to its overheating [12]. Thus, this amplitude should have optimal range of changing. For fibers and capillaries (inclusive the multi-crystal fibers pulling), this range is

Figure 17.
Sapphire rod of 10 mm in outer diameter with capillary channel of 450 μm.
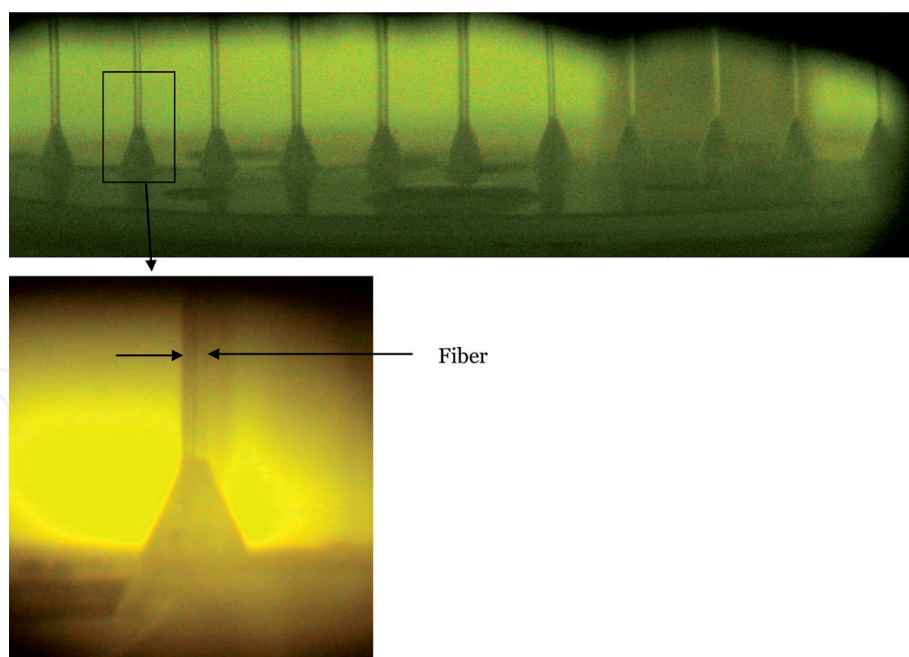
Figure 18.
Sapphire fibers of 150–300 μm in diameter grown by multi-crystal growth process.

sufficiently narrow. The need of maintaining the narrow range of these oscillations' amplitude requires the use of the second control loop tuning the first PID loop by the appropriate change of the programmed radius of the crystal or middle radii of the crystals in multi-crystal pulling.

An example of the automated growth of the capillary channel in the body of the bulk crystal is demonstrated in **Figure 17**.

Figure 18 shows sapphire fibers of 150–300 μm in diameter, which have been grown by multi-crystal process (up to 100 crystals per one process).

8. Conclusion

Comparable analysis of the forms and behaviors of the menisci profile curves for various signs of the boundary angle θ_d featuring the cases of ordinary (planar) and sloped working surfaces of the dies was made using the numerical analysis of the Young-Laplace capillary equation.

Calculation of the second derivatives of the menisci profile curves allowed us to analyze the curvature of the menisci profiles and observe its bulges.

Analysis of the inner and outer circular menisci has shown some different heights and behaviors of these menisci profiles because of the different signs of the azimuthal curvatures in the capillary equation.

Using numerical solution of the Young-Laplace capillary equation, the parameters for observing expression for automated growth control for tubular crystals as well as for capillaries and fibers were found. The sapphire tubes, capillaries, and fibers of good quality have been grown using automated system of control.

Acknowledgements

Author details

Sergei N. Rossolenko[1*], Gleb M. Katyba[1,2], Irina N. Dolganova[1,2],
Irina A. Shikunova[1], Dmitry O. Stryukov[1], Kirill I. Zaitsev[2,3]
and Vladimir N. Kurlov[1]

1 Institute of Solid State Physics RAS, Moscow, Russia

2 Bauman Moscow State Technical University, Moscow, Russia

3 Prokhorov General Physics Institute of the Russian Academy of Sciences, Moscow,
Russia

*Address all correspondence to: ross@issp.ac.ru

IntechOpen

References

[1] Sapphire KVN. Properties, growth, and applications. In: Hashmi S, editor. Reference Module in Materials Science and Materials Engineering. Oxford: Elsevier; 2016. pp. 1-11. DOI: 10.1016/B978-0-12-803581-8.03681-X

[2] Chalmers B, LaBelle HE, Mlavsky AI. Edge-defined, film-fed crystal growth. Journal of Crystal Growth. 1972;**13/14**:84-87. DOI: 10.1016/0022-0248(72)90067-X

[3] Stepanov AV. Future of Metal Working. Leningrad: Lenizdat; 1963. p. 130

[4] LaBelle HE. EFG, the invention and application to sapphire growth. Journal of Crystal Growth. 1980;**50**:8-17. DOI: 10.1016/0022-0248(80)90226-2

[5] Kurlov VN, Rossolenko SN, Abrosimov NV, Lebbou KH. Shaped crystal growth. In: Th D, editor. Crystal Growth Processes Based on Capillarity Czochralski, Floating Zone, Shaping and Crucible Techniques. Chichester, West Sussex, United Kingdom: John Wiley & Sons Ltd; 2010. pp. 277-354. DOI: 10.1002/9781444320237.ch5

[6] Antonov PI, Kurlov VN. A review of developments in shaped crystal growth of sapphire by the Stepanov and related techniques. Progress in Crystal Growth and Characterization of Materials. 2002;**44**:63-122. DOI: 10.1016/S0960-8974(02)00005-0

[7] Shikunova IA, Stryukov DO, Rossolenko SN, Kiselev AM, Kurlov VN. Neurosurgery contact handheld probe based on sapphire shaped crystal. Journal of Crystal Growth. 2017;**457**:265-269. DOI: 10.1016/j.jcrysgro.2016.08.062

[8] Zaytsev KI, Katyba GM, Kurlov VN, Shikunova IA, Karasik VE, Yurchenko SO. Terahertz photonic crystal waveguides based on sapphire shaped crystals. IEEE Transactions on Terahertz Science and Technology. 2016;**6**(4):576-582. DOI: 10.1109/TTHZ.2016.2555981

[9] Katyba GM, Zaytsev KI, Chernomyrdin NV, Shikunova IA, Komandin GA, Anzin VB, et al. Sapphire photonic crystal waveguides for terahertz sensing in aggressive environments. Advanced Optical Materials. 2018;**6**:1800573. DOI: 10.1002/adom.201800573

[10] Katyba GM, Zaytsev KI, Dolganova IN, Shikunova IA, Chernomyrdin NV, Yurchenko SO, et al. Sapphire shaped crystals for waveguiding, sensing and exposure applications. Progress in Crystal Growth and Characterization of Materials. 2018;**64**:133-151. DOI: 10.1016/j.perysgrow.2018.10.002

[11] Kurlov VN, Rossolenko SN. Growth of shaped sapphire crystals using automated weight control. Journal of Crystal Growth. 1997;**173**:417-426. DOI: 10.1016/S0022-0248(96)00836-6

[12] Abrosimov NV, Kurlov VN, Rossolenko SN. Automated control of Czochralski and shaped crystal growth processes using weighing techniques. Progress in Crystal Growth and Characterization of Materials. 2003;**46**:1-57. DOI: 10.1016/S0960-8974(03)90001-5

[13] Tsivinnski SV. Application of the theory of capillary phenomena to obtain products of a given shape directly from the melt by A.V. Stepanov method. Inzhenerno-fizichesky Zhurnal. 1962;**5**:59-65. (in Russian)

[14] Tatarchenko VA. Shaped Crystal Growth. Dordrecht: Kluwer Academic Publishers; 1993. p. 287

[15] Schelkin YF. Determining the shape of the column during the growth

of single crystals by the Czochralski method from a melt with a free surface. Fizika i Khimija Obrabotki Materialov. 1971;**3**:29-33. (in Russian)

[16] Surek T, Chalmers B, Mlavsky AI. The edge-defined film-fed growth of controlled shape crystals. Journal of Crystal Growth. 1977;**42**:453-465. DOI: 10.1016/0022-0248(77)90231-7

[17] Kuandykov LL, Antonov PI. Shaped melt column optimal choice on the basis of an equilibrium growth angle value. Journal of Crystal Growth. 2001;**222**:852-861. DOI: 10.1016/S0022-0248(00)01010-1

[18] Rossolenko SN. Menisci masses and weights in Stepanov (EFG) technique: Ribbon, rod, tube. Journal of Crystal Growth. 2001;**231**:306-315. DOI: 10.1016/S0022-0248(01)01448-8

[19] Satunkin GA, Rossolenko SN. Analysis of the dynamics of the controlled crystallization process using the Czochralski method. Crystal Research and Technology. 1986;**21**:1125-1138. DOI: 10.1002/crat.2170210902

[20] Red'kin BS, Kurlov VN, Pet'kov IS, Rossolenko SN. Investigation of the crystal growth conditions of gadolinium molybdate crystals. Journal of Crystal Growth. 1990;**104**:77-79. DOI: 10.1016/0022-0248(90)90310-H

[21] Rossolenko SN, Zhdanov AV. Equilibrium shapes of liquid menisci subjected to gravity force and surface tension. Journal of Crystal Growth. 1990;**104**:8-13. DOI: 10.1016/0022-0248(90)90300-A

[22] Landau LD, Lifshitz EM. Mehanika Splosnih Sred. Moscow: Gostehteorizdat; 1953. p. 788

[23] Satunkin GA. Determination of growth angles, wetting angles, interfacial tensions and capillary constant values of melts. Journal of Crystal Growth. 2003;**255**:170-189. DOI: 10.1016/S0022-0248(03)01187-4

[24] Ettouney HM, Brown RA, Kalejs JP. Analysis of operating limits in edge-defined film-fed crystal growth. Journal of Crystal Growth. 1983;**62**:230-246. DOI: 10.1016/0022-0248(83)90301-9

[25] Thomas PD, Ettouney HM, Brown RA. A thermal-capillary mechanism for a growth rate limit in edge-defined film-fed growth of silicon sheets. Journal of Crystal Growth. 1986;**76**:339-351. DOI: 10.1016/0022-0248(86)90380-5

[26] Thomas PD, Brown RA. Rate limits in silicon sheet growth: The connections between vertical and horizontal methods. Journal of Crystal Growth. 1987;**82**:1-9. DOI: 10.1016/0022-0248(87)90157-6

[27] Derby JJ, Brown RA. On the dynamics of Czochralski crystal growth. Journal of Crystal Growth. 1987;**83**:137-151. DOI: 10.1016/0022-0248(87)90514-8

[28] Lan CW. Thermal-capillary analysis of floating-zone growth of tube crystals: Steady-state and condition dominated calculations. Journal of Crystal Growth. 1994;**135**:606-618. DOI: 10.1016/0022-0248(94)90154-6

[29] Yeckel A, Salinger AG, Derby JJ. Theoretical analysis and design considerations for float-zone refinement of electronic grade silicon sheets. Journal of Crystal Growth. 1995;**152**:51-64. DOI: 10.1016/0022-0248(95)00088-7

[30] Roy A, Zhang H, Prasad V, Mackintosh B, Quellette M, Kalejs JP. Growth of large diameter silicon tube by EFG technique: Modeling and experiment. Journal of Crystal Growth. 2001;**230**:224-231. DOI: 10.1016/S0022-0248(01)01327-6

[31] Satunkin GA, Tatarchenko VA. Shape analysis and meniscus height calculations for various types of capillary shaping. Journal of Colloid and Interface Science. 1985;**104**:318-333. DOI: 10.1016/0021-9797(85)90042-6

[32] Zhdanov AV, Satunkin GA, Ponomareva RP. Stability of liquid menisci. Journal of Colloid and Interface Science. 1985;**104**:334-343. DOI: 10.1016/0021-9797(85)90043-8

[33] Kurlov VN, Epelbaum BM. Fabrication of near-net-shaped sapphire domes by noncapillary shaping method. Journal of Crystal Growth. 1997;**179**:175-180. DOI: 10.1016/S0022-0248(97)00111-5